

RotLES: A Rotorcraft-based Lattice Boltzmann LES code for Rapid Analysis and Design Space Exploration

*Nicholas Peters
Ames Research Center, Moffett Field, California*

NASA STI Program . . . in Profile

Since its founding, NASA has been dedicated to the advancement of aeronautics and space science. The NASA scientific and technical information (STI) program plays a key part in helping NASA maintain this important role.

The NASA STI Program operates under the auspices of the Agency Chief Information Officer. It collects, organizes, provides for archiving, and disseminates NASA's STI. The NASA STI Program provides access to the NASA Aeronautics and Space Database and its public interface, the NASA Technical Report Server, thus providing one of the largest collections of aeronautical and space science STI in the world. Results are published in both non-NASA channels and by NASA in the NASA STI Report Series, which includes the following report types:

- **TECHNICAL PUBLICATION.** Reports of completed research or a major significant phase of research that present the results of NASA programs and include extensive data or theoretical analysis. Includes compilations of significant scientific and technical data and information deemed to be of continuing reference value. NASA counterpart of peer-reviewed formal professional papers, but having less stringent limitations on manuscript length and extent of graphic presentations.
- **TECHNICAL MEMORANDUM.** Scientific and technical findings that are preliminary or of specialized interest, e.g., quick release reports, working papers, and bibliographies that contain minimal annotation. Does not contain extensive analysis.
- **CONTRACTOR REPORT.** Scientific and technical findings by NASA-sponsored contractors and grantees.

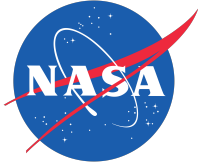
- **CONFERENCE PUBLICATION.** Collected papers from scientific and technical conferences, symposia, seminars, or other meetings sponsored or co-sponsored by NASA.
- **SPECIAL PUBLICATION.** Scientific, technical, or historical information from NASA programs, projects, and missions, often concerned with subjects having substantial public interest.
- **TECHNICAL TRANSLATION.** English-language translations of foreign scientific and technical material pertinent to NASA's mission.

Specialized services also include creating custom thesauri, building customized databases, and organizing and publishing research results.

For more information about the NASA STI Program, see the following:

- Access the NASA STI program home page at <http://www.sti.nasa.gov>
- E-mail your question to help@sti.nasa.gov
- Fax your question to the NASA STI Information Desk at 443-757-5803
- Phone the NASA STI Information Desk at 443-757-5802
- Write to:
STI Information Desk
NASA Center for AeroSpace Information
7115 Standard Drive
Hanover, MD 21076-1320

NASA/TM-20250007146



RotLES: A Rotorcraft-based Lattice Boltzmann LES code for Rapid Analysis and Design Space Exploration

*Nicholas Peters
Ames Research Center, Moffett Field, California*

National Aeronautics and
Space Administration

Ames Research Center
Moffett Field, California 94035

July 2025

Acknowledgments

The author express his gratitude to Carlos Malpica and Michael Radotich for their valuable feedback in reviewing this paper.

The use of trademarks or names of manufacturers in this report is for accurate reporting and does not constitute an official endorsement, either expressed or implied, of such products or manufacturers by the National Aeronautics and Space Administration.
--

Available from:

NASA Center for AeroSpace Information
7115 Standard Drive
Hanover, MD 21076-1320

National Technical Information Service
5301 Shawnee Road
Alexandria, VA 22312

Available electronically at <http://www.sti.nasa.gov>

RotLES: A Rotorcraft-based Lattice Boltzmann LES code for Rapid Analysis and Design Space Exploration

Nicholas Peters
National Aeronautics and Space Administration
Ames Research Center
Moffett Field, California 94035

Summary

In this NASA-TM, an overview is provided of an exploratory study into developing an LBM rotorcraft based LES tool called RotLES. Approaches explored in the RotLES code are designed to allow for rapid analysis and design space exploration all within the context of a user-friendly, minimal setup required framework. In RotLES, handling of solid body geometries and rotor modeling is designed to require minimal user setup, thus allowing for rapid case generation. Solid body geometries can be modeled automatically from a user provided STL file. Rotor modeling is handled through either actuator disk or actuator line source term modeling, both being defined using rotor definitions commonly available in both early stages conceptual and preliminary vehicle design. To enable rapid analysis with large scale grids, RotLES is coded using the NVIDIA CUDA language with CUDA aware OpenMPI. The inclusion of multi-GPU processing allows for scalable and rapid case turn around, allowing for multi-rotor unsteady simulations with billions of lattices to run in just a few hours. For validation of the RotLES model, outwash predictions for a single rotor are presented. Results showed RotLES closely tracks blade-resolved OVERFLOW predictions while greatly reducing overall computational expense. In closing remarks, a list of suggested future work is provided.

Nomenclature

ADM	Actuator Disk Modeling
ALM	Actuator Line Modeling
BGK	Bhatnagar-Gross-Krook
CPU	Central Processing Unit
GPU	Graphical Processing Unit
LBM	Lattice Boltzmann Method
LES	Large Eddy Simulation
NASA	National Aeronautics and Space Administration
RVLT	Revolutionary Vertical Lift Technology
STL	Stereolithography

Variables

A_{PAXman}	PAXman cross-sectional area
cx_i	x-direction lattice component
cy_i	y-direction lattice component
cz_i	z-direction lattice component
C_s	Smagorinsky constant
F	force
f_i	LBM particle density function
F_{PAXman}	PAXman force
L	reference length
Re	Reynolds number
S	stress tensor
t	time
U	reference velocity
u	x-axis velocity
v	y-axis velocity
w	z-axis velocity
w_i	lattice component weighting
ν_{eff}	effective viscosity
ν_o	laminar viscosity
ν_t	turbulent viscosity
ρ	density
τ	time relaxation factor
τ_{les}	les corrected time relaxation factor
Ω_j	solid angle

1 Introduction

In the of Spring 2025, an effort was started within the National Aeronautics and Space Administration (NASA) Revolutionary Vertical Lift Technology (RVLT) project to explore the feasibility of establishing a rotorcraft-based Large Eddy Simulation (LES) tool for rapid analysis and design space exploration. This tool, tentatively called RotLES (short for Rotorcraft-LES), was to be a Lattice Boltzmann Method (LBM) based simulation tool and capable of scaling to multiple GPUs, thus allowing for rapid high-fidelity predictions for rotorcraft relevant cases such as outwash, downwash, rotor-rotor interference, rotor-fuselage interference, and large scale urban flow turbulence predictions. The development of this tool was encouraged by findings well established in the literature which highlight the broad impact LBM may have in the rotorcraft field (Ref. 1–4). In this NASA Technical Memorandum (NASA-TM), a summary will be provided of the developed tool, including methodologies used, a preliminary validation of the tool, and a list of future recommendations.

2 Methodology

In this section, a summary is provided for all numerical approaches currently implemented in RotLES. First, an overview of the selected LBM implementation will be provided, including discretization approach, LES subgrid modeling, and boundary conditions used. Implementation of the CAD processing and rotor modeling will then be discussed. Finally, a brief discuss of the GPU and multi-GPU implementation of the code will be provided.

2.1 Lattice Boltzmann Method

To enable the rapid simulation of large-scale turbulent wakes, the Lattice Boltzmann Method (LBM) was chosen as the foundational algorithm for the RotLES code. Unlike traditional Navier-Stokes solvers that directly evolve macroscopic flow variables such as density, velocity, and pressure, LBM models fluid motion through the evolution of a particle distribution function, f_i , which is a function of both velocity, time, and space. This function, f_i , represents the probability of finding particles with a given velocity at each point in space and time. One simplified analogy commonly used for LBM is to think of f_i in terms of cars in traffic. The variable f_i can be thought as representing cars moving north, south, east and west at a given intersection. If we sum all directions of f_i , we'll find the total number of cars at the intersection. But if we sum cars moving west and east, we'll find the total number of cars moving in the west or east direction. Similarly, summing all components of f_i in LBM will result in local density, while summing f_i along any given x, y, or z-axis direction will result in momentum in a given direction. Fluid behavior emerges from the repeated streaming (updating particle positions) and collision (computing particle equilibrium), providing a highly parallelizable and efficient framework well-suited for simulating complex turbulent flows.

A key aspect of the LBM approach lies in its unique discretization strategy. In LBM, the computational domain is divided into a regular grid, and at each grid point, fluid particles can travel along a discrete set of velocity directions, known as a lattice. These discrete directions define how particles stream from one node to another during each time step. While multiple lattice configurations exist, RotLES employs the commonly used D3Q19 lattice, which defines 19 discrete velocity vectors in a three-dimensional space. Particle collision is then modeled using the

Bhatnagar-Gross-Krook (BGK) collision model (Ref. 5). This structure balances computational efficiency and accuracy, making it well-suited for simulating turbulent flows. Figure 1 shows a visual of the D3Q19 lattice structure, visualizing the 19 discrete directions of f_i .

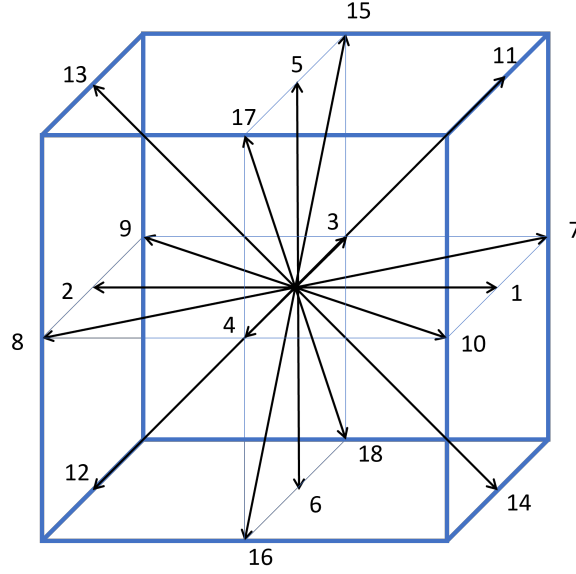


Figure 1.—Visualization of D3Q19 lattice used in RotLES.

2.1.1 Lattice Boltzmann Equations

To extract density and momentum from the particle density function, Eqns. 1 - 4 are used. In Equation 1, a summation is completed for all 19 directions of f_i to compute the density at a given lattice. In Equations 2 - 4, a similar summation is completed, but with new directional terms (cx_i, cy_i, cz_i) accounting for directionality of all 19 components of f_i .

$$\rho = \sum_i f_i \quad (1)$$

$$\rho u = \sum_i cx_i f_i \quad (2)$$

$$\rho v = \sum_i cy_i f_i \quad (3)$$

$$\rho w = \sum_i cz_i f_i \quad (4)$$

Once particle density and momentum are computed, Eqns. 5 - 6 are used to compute the equilibrium of f_i . In Equation 6, w_i is a lattice weighting variable and V is the velocity magnitude at the given lattice.

$$\beta = 3(cx_i u + cy_i v + cz_i w) \quad (5)$$

$$f_i^{eq} = w_i \rho \left(1 + \beta + 0.5 * \beta^2 - 1.5 V^2 \right) \quad (6)$$

After computing the equilibrium of f_i , f_i can be updated using Eqn. 7. In Equation 7, τ is the time relaxation factor, computed from user defined Reynolds number, reference velocity, and time step. Calculation of τ is shown in 8 where U is reference velocity, L is reference length, c_s is lattice speed of sound, δt is time step, and Re is Reynolds number.

$$f_i^{new} = f_i^{old} - \frac{f_i^{old} - f_i^{eq}}{\tau} \quad (7)$$

$$\tau = \frac{UL}{c_s^2 \delta t Re} + \frac{1}{2} \quad (8)$$

For stability purposes, the relaxation time τ is typically constrained to values of 0.6 or higher with a lower stability limit of 0.5. However, as shown in Eqn. 8, as the Reynolds number increases, τ decreases rapidly, approaching the lower stability limit of the LBM algorithm. Consequently, traditional LBM approaches have been limited to low Reynolds number applications, restricting their use in rotorcraft-relevant simulations.

2.1.2 LES Sub-grid Model

By incorporating a LES sub-grid model, however, the LBM method can be effectively extended to Reynolds numbers representative of practical, high-Reynolds, subsonic rotorcraft flows. To apply the LES sub-grid model, the turbulent eddy viscosity, ν_t must be computed. To compute ν_t , the shear stress tensor, S , must first be computed. After computing the tensor, the magnitude can be computed follow Eqn. 9.

$$S_{mag} = \sqrt{2(S_{xx}^2 + S_{yy}^2 + S_{zz}^2 + 2(S_{xy}^2 + S_{xz}^2 + S_{yz}^2))} \quad (9)$$

Using S_{mag} and the Smagorinsky constant, C_s , the turbulent eddy viscosity can then be computed using Eqn. 10. After computing ν_t and ν_o the a new effective viscosity ν_{eff} can be computed using Eqn. 12. After computing ν_{eff} , a new effective LES correct time relaxation factor can be computed for the given lattice using Eqn. 13.

$$\nu_t = C_s^2 S_{mag} \quad (10)$$

$$\nu_o = 1/3(\tau - 0.5) \quad (11)$$

$$\nu_{eff} = \nu_o + \nu_t \quad (12)$$

$$\tau_{les} = 3\nu_{eff} + 0.5 \quad (13)$$

2.2 Boundary Condition

2.2.1 Cartesian Block Boundary Conditions

For simplicity, in the current implementation of the code, Eqns. 1 - 13 are applied to a single Cartesian block grid. A total of 4 boundary conditions can be applied to either face of this block grids, namely: no-slip wall, symmetry, zero-gradient outflow, and Zou-He velocity inlet. For the

no-slip wall condition, a simple bounce back approach is used in which particle density function directions are inverted, there by enforcing the no slip condition. In addition to these four boundary conditions, solid-body and rotor modeling boundary conditions can be specified by the user.

2.2.2 Solid-Body Modeling

In the RotLES code, users have the option of specifying a solid-body, such as a building or fuselage, through use of a single STL input file. This user defined STL file is read into the RotLES code at startup, after which the solid angle formula (as shown in Eqn. 14) is used. In Equation 14, variables A, B, C are the respective distances from a given lattice location to the three vertices of a given triangle in the STL and Ω_j is the solid angle between the given lattice, j , and a given triangle in the STL. By using Equation 14, for each lattice in the computational domain a summation of Ω_j can be computed. If the summation of Ω_j is equal to 4π , then the given lattice is bounded by the given STL file. If the summation of Ω_j is not equal to 4π , then the given lattice is not bounded by the given STL.

$$\Omega_j = 2\tan^{-1} \left(\frac{|A \cdot (B \times C)|}{ABC + A(B \cdot C) + B(A \cdot C) + C(A \cdot B)} \right) \quad (14)$$

Internally to the code, this information is accounted for through a blanking variable, where values of 1 mean a lattice is inside the STL geometry, and a value of 0 means the lattice is outside the STL geometry. If the blanking is equal to 1, then a simple bounce back boundary condition is applied. While this wall modeling approach is quite simple, it does allow for the rapid, automatic modeling of bluff body geometries. For visualization, Fig. 2 shows a demonstration case for a RotLES simulation of simple drone fuselage.

$$blanking = \begin{cases} 1 & \text{if } \Omega = 4\pi \\ 0 & \text{if } \Omega \neq 4\pi \end{cases} \quad (15)$$

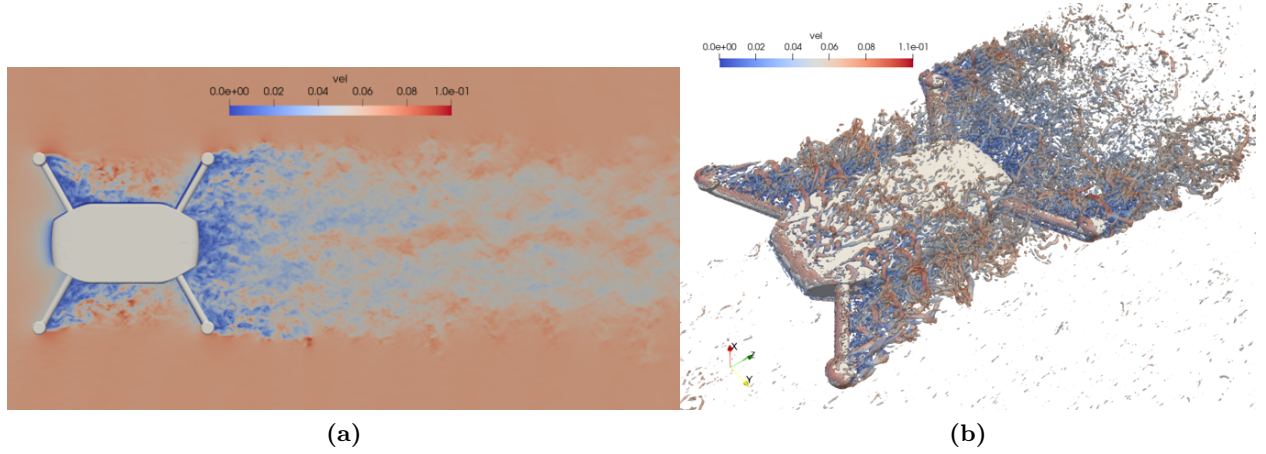


Figure 2.—Demonstration simulation for wake around a drone in 60 knots wind using a 1.5 billion cell mesh. Left graphic shows a $y = 0$ plane cut contoured by velocity magnitude, while right graphic shows iso-surfaces of q -criteria contoured by velocity magnitude.

2.2.3 Rotor Modeling

In the current implementation, two rotor momentum source term modeling approaches are implemented. Namely, these approaches are actuator disk modeling (ADM) and actuator line modeling (ALM). In both approaches source terms are based on implementation outlined by Asmuth, Henrik, et al. (Ref. 6), wherein body forces are simply modeled by shifting the momentum frame of reference as shown in Eqn. 16. In Equation 16, u is the velocity vector, Δt is the lattice time step, ρ is density, and F is the body force vector.

$$u = u + \frac{\Delta t}{2\rho} F \quad (16)$$

To compute the body forces, either an underlying Blade Element Theory (BET) model can be referenced or rotor loading can be prescribed. If a BET model is referenced, induced velocities must first be sampled for the LBM flow field. To extract induced velocities, series of flow field sensors near the rotor are prescribed. In the case of the rotor disk model, 20 evenly spaced radial and azimuth sensors are specified, for a total of 400 sensors. In the case of the ALM, 20 evenly spaced radial sensors are placed for each node. At each iteration, cells bounding the sensors are identified, after which a linear interpolation is used to compute the induced velocity. After finding the induced velocities, an underlying BET model can be used to compute the loading coefficients at each sensor location. A visualization of the sensor distribution is provided in Fig. 3.

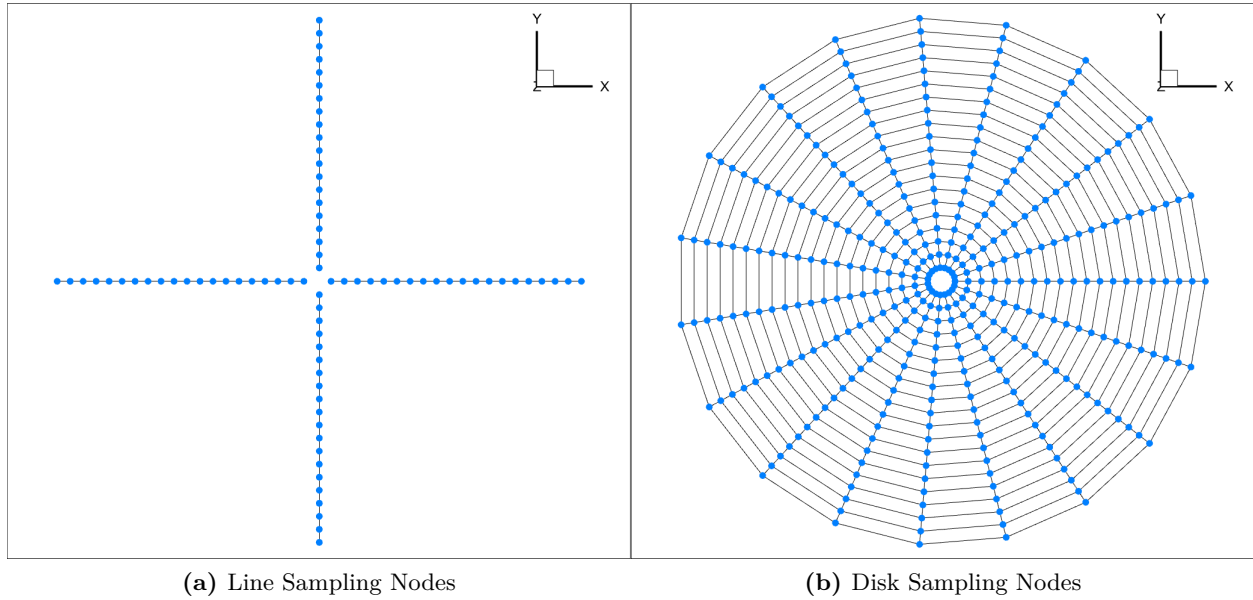


Figure 3.—Top down visual of wake sampling nodes when using the ADM (right) and ALM (left) models.

After computing the body force terms, it is necessary to identify the lattice nodes in the vicinity of the rotor model where these forces will be applied. For the ADM, this identification is performed through a two-step process. First, for each lattice position, the vertical distance from the rotor disk plane is calculated. If this distance is less than half the mean chord length, the radial distance from the lattice point to the rotor hub is then computed and compared to the rotor radius. If both criteria are satisfied, the lattice node is marked for source term addition. A similar procedure is followed for the ALM. However, in this case, an additional criterion is applied: the lattice must lie within a distance of 0.5 times the mean chord length in the chord-wise direction relative to the blade at the given time step.

Once the relevant lattice nodes are identified, an inverse distance interpolation is used to determine the appropriate body force values from the reference sample points. As currently implemented, users can specify either line or disk rotor models. As a demonstration, a simple example of a quad rotor configuration in forward flight is provided in Figs. 4 and 5. Users further have the ability to model rotors not just in isolation, but in the presences of any user defined STL file, thus allowing for rapid analysis of rotorcraft relevant cases, such the case of rotor's in urban settings Fig. 6.

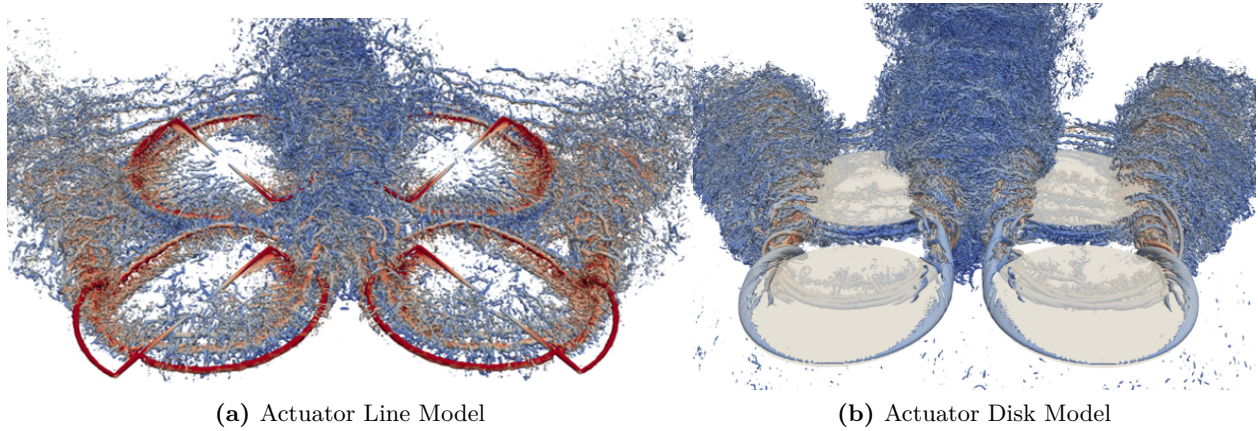


Figure 4.—Demonstration simulation of a quad-rotor configuration in forward flight. Left graphic shows modeling using ALM, while right graphic shows modeling using ADM. Both graphics show iso-surfaces of q -criteria contoured by velocity magnitude.

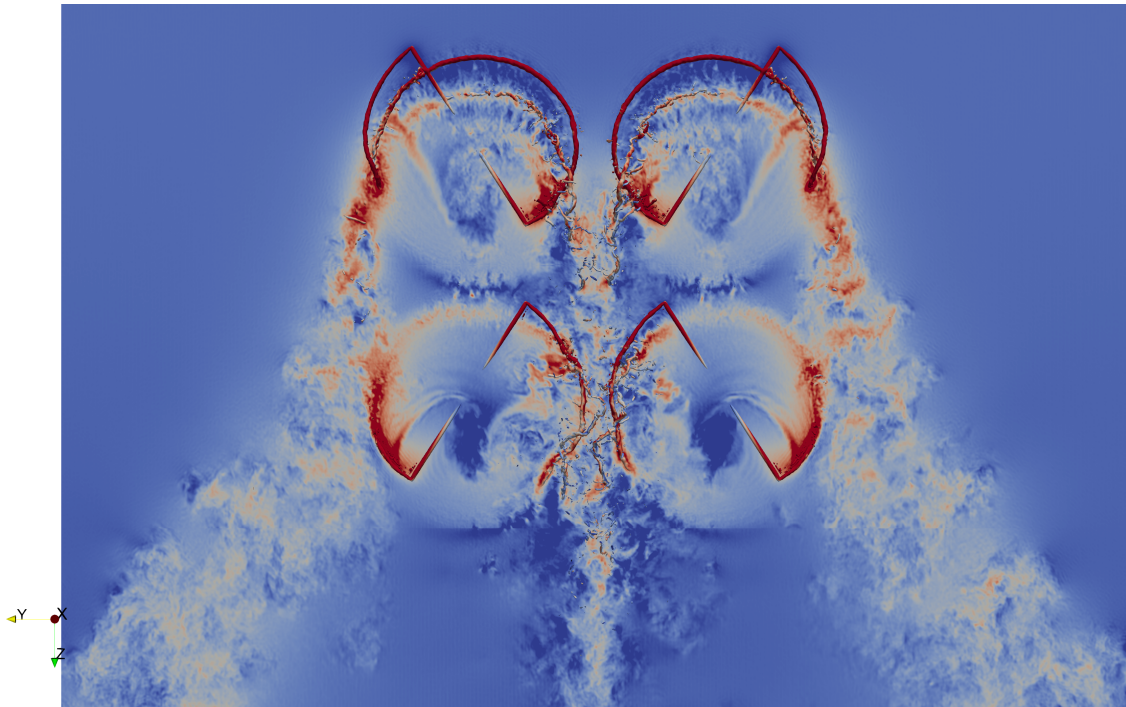


Figure 5.—Demonstration ALM simulation of a quad-rotor configuration in forward flight. Graphic shows a $x = 0$ plane cut contoured by velocity magnitude where the x -axis is inline with the rotor's thrust axis.

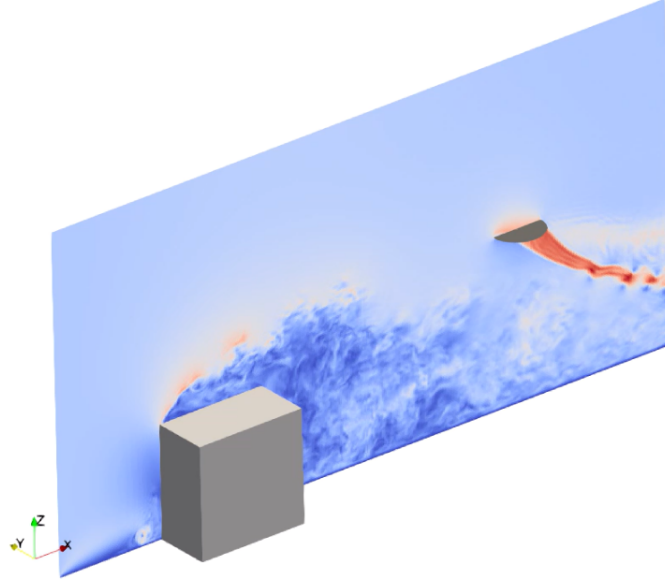


Figure 6.—Demonstration simulation of a rotor hovering behind a building in 40 knots of wind. Graphic shows a $y = 0$ plane cut contoured by velocity magnitude.

2.3 GPU Computing

One notable limitation of the current LBM implementation is its reliance on a single, uniform Cartesian block grid. This constraint becomes particularly significant in rotorcraft applications, where large computational domains are often required, such as modeling multi-rotor vehicles operating in urban environments. In such cases, the total number of grid points can easily reach hundreds of millions or even billions, rendering CPU-based simulations computationally prohibitive, even when using thousands of cores.

However, thanks to recent advancements in GPU hardware and the inherently parallel nature of the LBM algorithm, simulations of this scale can now be efficiently executed on modern GPUs. To leverage this capability, the RotLES code was implemented in C using a series of CUDA kernels, enabling compatibility with most NVIDIA GPUs. With an in-place streaming strategy, RotLES running on a single NVIDIA A100-80GB GPU is capable of simulating 0.5 billion lattice nodes for 100,000 time steps in under six hours.

To scale further, CUDA-aware OpenMPI was integrated, allowing RotLES to efficiently model cases involving several billion lattice nodes while maintaining fast turnaround times. As a demonstration, Figure 7 shows 60-knot flow around a building, simulated using 1.5 billion lattice points. Using just four NVIDIA A100 GPUs, the time required to develop a time-periodic wake and extract flow fields for sampling was approximately five hours. Provided the relatively low computational cost and quick turn around time, the LBM-LES approach appears to be a viable method for rapid high-fidelity predictions in both conceptual and preliminary design applications.

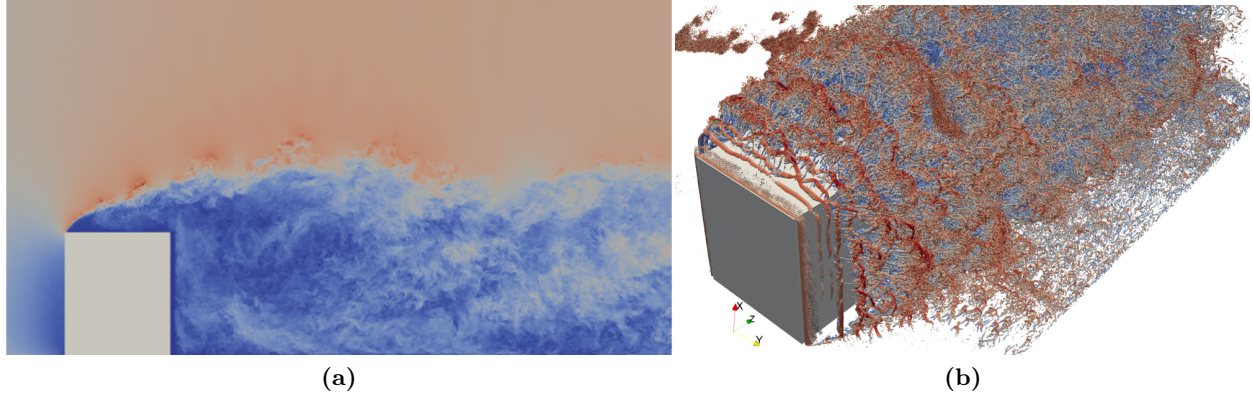


Figure 7.—Demonstration simulation for wake around a building in 60 knots wind using a 1.5 billion cell mesh. Left graphic shows a $y = 0$ plane cut contoured by velocity magnitude, while right graphic shows iso-surfaces of q -criteria contoured by velocity magnitude.

3 Validation

In this section, a preliminary validation of the RotLES code will be presented. The objective of this validation effort is to both validate the implemented LBM rotor disk model and demonstrate a practical use-case of the LBM code. Case setup will first be reviewed after which a summary of computational cost and modeling fidelity will be provided.

3.1 Case Setup

This study focuses efforts on evaluating the derived LBM model for a single case of rotor outwash. The case of interest is based on experimental measurements as reported by Silva and Riser (Ref. 7). In this experiment, a series of outwash measurements were recorded for a CH-47D hovering in ground effect (IGE) at varying disk loading and altitudes. Results published by Ramasamy and Yamauchi (Ref. 8) demonstrated that outwash characteristics of a single rotor match well with the outwash in the forward region of a CH-47D. As such, in this study, single rotor outwash predictions are compared against full scale outwash measurements in the forward region of a CH-47D as reported by Silva and Riser. In Silva and Riser’s experiment, a full-scale CH-47D was hovering at a rotor height of 0.578 diameters and with a thrust coefficient of 0.0061. Measurements were then taken at azimuth locations of 0° , 90° , 180° , and 270° and radial locations ranging from 24 to 180 feet. For the single rotor IGE case, measurements reported at an azimuth of 0° was used. For benchmarking, results from this study are compared against the outwash predictions reported by Peters and Shirazi (Ref. 9) using three different methods, namely OVERFLOW-CFD blade-resolved, OVERFLOW-CFD actuator line, and CHARM-based comprehensive analysis predictions.

To simulate this configuration, a single actuator disk was modeled hovering in ground effect (IGE) at a height of 0.578 rotor diameters, with a constant thrust coefficient of 0.0061. The computational domain was discretized using a single Cartesian block mesh consisting of 800 nodes in both the x and y directions, and 266 nodes in the z direction—yielding a total of approximately 170 million lattice nodes. Zero-gradient boundary conditions were applied on the positive and

negative x/y boundaries, as well as the positive z boundary. A slip-wall boundary condition was imposed on the negative z boundary to represent the ground surface.

For comparison of modeling fidelity, two metrics were used. The first metric shows time averaged boundary layer extracts at 6 radial distances from the rotor’s hub ranging from 1 radii to 2 diameters from the rotor’s hub. In addition to comparing rotor outwash velocity profiles, outwash predictions using each numerical approach are compared using the PAXman model. The PAXman model is an anthropometric model used to compute forces on representative ground personnel. To use the PAXman model, outwash boundary layer is integrated up to a height of 5.5 feet using Eqn. 17 and represent the force on a 6-ft PAXman crouched and leaning while immersed in outwash. In Equation 17, F_{PAXman} is the predicted force on ground personnel, u is the outwash velocity, and dA_{pax} is the incremental frontal area of the ground personnel crouched and leaning in the outwash.

$$F_{PAXman} = \int \frac{1}{2} \rho u^2 dA_{pax} \quad (17)$$

3.2 Results and Discussion

The LBM simulation was executed on a single NVIDIA A100 GPU, requiring approximately one hour to generate a time-periodic wake and collect sufficient data for time-averaged analysis. Table 1 summarizes the relative computational costs of all four approaches. The results clearly demonstrate that the LBM-based model offers substantial computational savings, in both runtime and hardware utilization, compared to the OVERFLOW-based CFD methods. Both OVERFLOW CFD approaches required several hundred CPUs, thus requiring use of large super-computing clusters. Yet, LBM was shown to run over an order of magnitude faster while utilizing hardware more accessible to a broader range of design teams. Additionally, while CHARM simulations may have achieved faster runtimes through fewer revs or additional case optimization, the LBM approach remains competitive in terms of run time. However, it is important to note that the LBM simulations were performed on significantly more expensive hardware than that used for CHARM.

With the baseline computational cost comparison established, the numerical fidelity of the LBM model can now be established. Figure 8 presents outwash boundary layer predictions from each numerical approach at 6 radial locations from the rotor hub, spanning the range $0.5 \leq r/D \leq 2$. Profiles are plotted up to a vertical height of 12 feet, corresponding to approximately $r/D = 0.2$. The results demonstrate that the LBM approach performs favorably when compared to experimental measurements, outwash predictions generally fall within the reported uncertainty bounds and closely follow experimental trends. Furthermore, the LBM model shows strong agreement with both OVERFLOW-based CFD approaches, with peak time-averaged outwash velocities and boundary layer profiles aligning well across methods.

To further assess the fidelity of the LBM model, the outwash flow field was integrated using the PAXman methodology. Figure 9 displays the resulting PAXman-integrated outwash predictions. Beyond a radial distance of approximately $r/D = 0.75$, the LBM and CFD predictions become nearly indistinguishable. Moreover, the LBM model maintains close agreement with experimental data, particularly beyond $r/D = 1$, consistently remaining within the experimental uncertainty bounds and capturing the mean trends with high accuracy. Provided the relative low computational cost of the LBM model compared to CFD, results of this study appears to show the LBM model may be a viable alternative to CFD for outwash predictions.

Table 1.—Comparison of approximate computational cost between blade-resolved, actuator line, CHARM, and LBM numerical approaches for single CH-47D rotor IGE.

Value	OVERFLOW Blade Resolved	OVERFLOW Actuator Line	CHARM	LBM
Hardware	1,440 CPUs	336 CPUs	8 CPUs	1 GPU
Hours	140	12	5	1

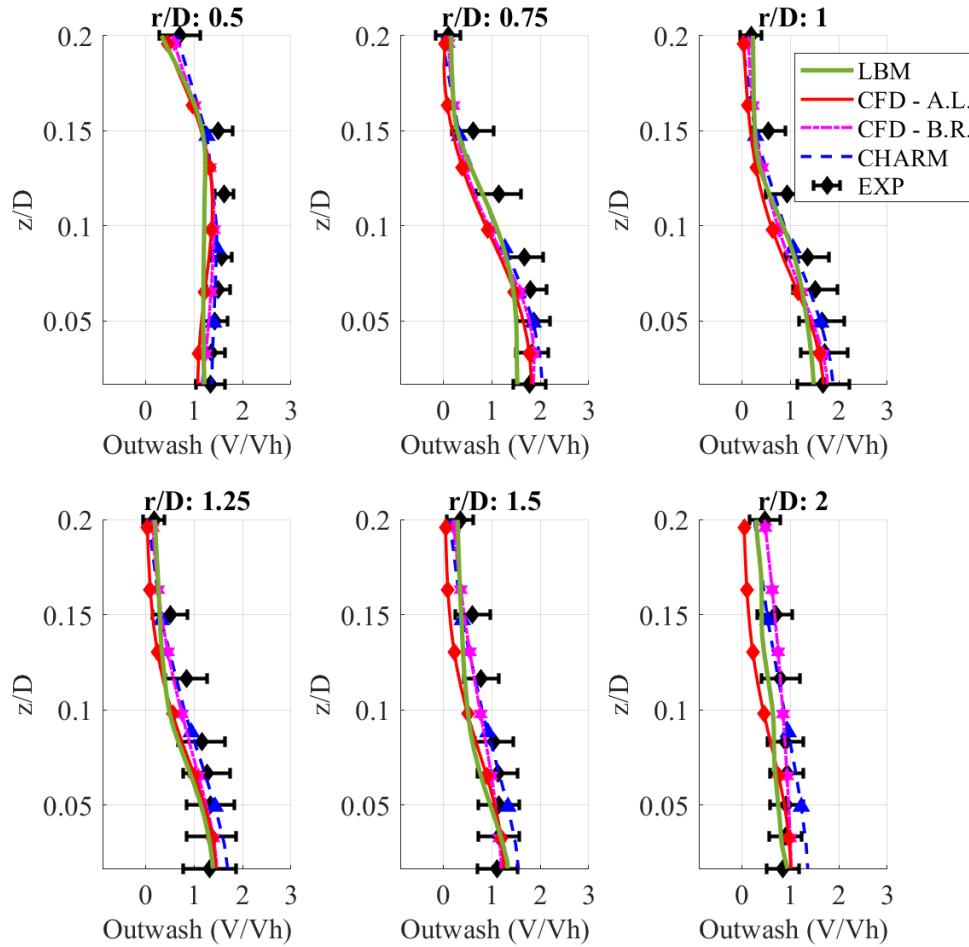


Figure 8.—Outwash boundary layer profiles compared between experiment and numerical simulations.

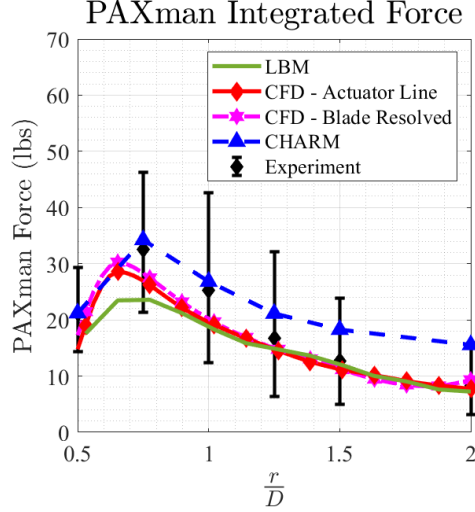


Figure 9.—PAXman integrated outwash compared between experiment and numerical simulations.

4 Future Work and Recommendations

It is important to highlight there are several limitations of the current RotLES code and its validation. For the RotLES code to become a practical tool for the rotorcraft community, these limitations must be overcome. Furthermore, findings of this paper, among others, has provided strong evidence that a well validated purpose built LBM code for the rotorcraft community may bring significant advantages over traditional CFD simulation tools. An abbreviated list of these limitations/future recommendations is provided below.

- A significant limitation of the RotLES code is its use of a single Cartesian block for grid generation. While this modeling simplification allowed for rapid code development and evaluation of the LBM method, it does greatly limit the code’s capability. To allow for the modeling of larger computational domains, future work must implement multi-block grid generation approaches. One such that has been shown to work well for LBM is Octree grid generation.
- The RotLES code currently uses a simple bounce back boundary condition for wall modeling. This simplistic approach provides no reasonable route for modeling of boundary layers of attached flows. As such, future work must focus on implementing a wall model to more accurately predict attached flows over geometries.
- In future work, an adaptive mesh refinement scheme should be included to more efficiently capture relevant flow features.
- Thus far, the RotLES code has been validated for single rotor outwash predictions. This preliminary study validates the implementation of the rotor disk model for wake predictions, and validates the LBM wake model. However, there still remains significant validation work that must be completed before solutions from the RotLES code can be practically used.

Further validation must include rotor performance predictions, rotor downloading, actuator disk multi-rotor outwash, actuator line single/multi-rotor outwash, bluff-body wake predictions, etc.

- To make the RotLES code more useful for the rotorcraft community, an API for comprehensive analysis coupling should be implemented.
- Further work should be taken to evaluate codes ability to approach near real-time predictions, thus making it a more useful tool for rotorcraft flight dynamics applications.

References

1. Thibault, S.; Holman, D.; Garcia, S.; and Trapani, G.: CFD Simulation of a quad-rotor UAV with rotors in motion explicitly modeled using an LBM approach with adaptive refinement. *55th AIAA aerospace sciences meeting*, 2017, p. 0583.
2. Romani, G.; and Casalino, D.: Rotorcraft blade-vortex interaction noise prediction using the Lattice-Boltzmann method. *Aerospace Science and Technology*, vol. 88, 2019, pp. 147–157.
3. Ashok, S. G.; Jude, D.; and Rauleder, J.: Comparison of Navier-Stokes and Lattice-Boltzmann Method CFD Approaches for Ship-Rotor Interactional Aerodynamics Using Cartesian GPU Solvers. *Transformative Vertical Flight 6th Decennial Aeromechanics Specialists' Conference*, 2024.
4. Ashok, S. G.; and Rauleder, J.: Real-Time Coupled Ship-Rotorcraft Interactional Simulations Using GPU-Accelerated Lattice-Boltzmann Method. *Journal of the American Helicopter Society*, vol. 70, no. 2, 2025, pp. 1–25.
5. Qian, Y.-H.; d'Humières, D.; and Lallemand, P.: Lattice BGK models for Navier-Stokes equation. *Europhysics letters*, vol. 17, no. 6, 1992, p. 479.
6. Asmuth, H.; Olivares-Espinosa, H.; Nilsson, K.; and Ivanell, S.: The actuator line model in lattice Boltzmann frameworks: numerical sensitivity and computational performance. *Journal of Physics: Conference Series*, IOP Publishing, vol. 1256, 2019, p. 012022.
7. Silva, M.; and Riser, R.: CH-47D Tandem Rotor Outwash Survey. *Proceedings of the 67th Annual American Helicopter Society Forum.*, Virginia Beach, Virginia, 2011.
8. Ramasamy, M.; and Yamauchi, G. K.: Using Model-Scale Tandem-Rotor Measurements in Ground Effect to Understand Full-Scale CH-47D Outwash. *Journal of the American Helicopter Society*, vol. 62, no. 1, 2017, pp. 1–14. URL <https://www.ingentaconnect.com/content/ahs/jahs/2017/00000062/00000001/art00004>.
9. Peters, N.; and Shirazi, D.: On the Application of an Actuator Line Model for Rotorcraft Outwash Predictions. *AIAA SciTech 2025 Forum*, 2025.
